Supporting Information

A Nonvacuum Approach for Fabrication of $Cu_2ZnSnSe_4/In_2S_3$ Thin Film Solar Cell and Optoelectronic Characterization

Dhruba B. Khadka, SeongYeon Kim, JunHo Kim*

Department of Physics, Incheon National University, 12-1 Songdo-dong Yeonsu-gu, 406-772 Incheon, South Korea

*** Correspondence**
E-mail: jhk@inu.ac.kr
Phone: +82-32-835-8221

Supporting data:

Table S1. Device parameters of the corresponding cells of Figure S2.

S1. Raman spectrum (a) and transmittance (b) of indium sulfide (In_2S_3) buffer deposited by chemical spray pyrolysis. Inset: (b) Tauc plot for band gap estimation. These results are in good agreement to the earlier reports. [1,2]

S2. J-V curves of devices fabricated by same conditions as those of best solar cell device.

S3. J-V-T characteristics of champion device under white light illumination (a) and dark condition (b) in the temperature range 300-90 K with $\Delta T = 10$ K as indicated by arrow points.

S4. J-V-T characteristics under different filtered light illuminations: (a) light with wavelengths higher than 665 nm, (b) light with wavelengths higher than 500 nm, and (c) light with wavelengths in between 275-375 nm. Arrow points towards lower temperature (T= 300-100 K; $\Delta T = 20$ K).

S5. Charge carrier density profile determined from capacitance voltage (C-V) measurement at 90 K. Inset: Mott-Schottky plot and built-in-potential estimation.

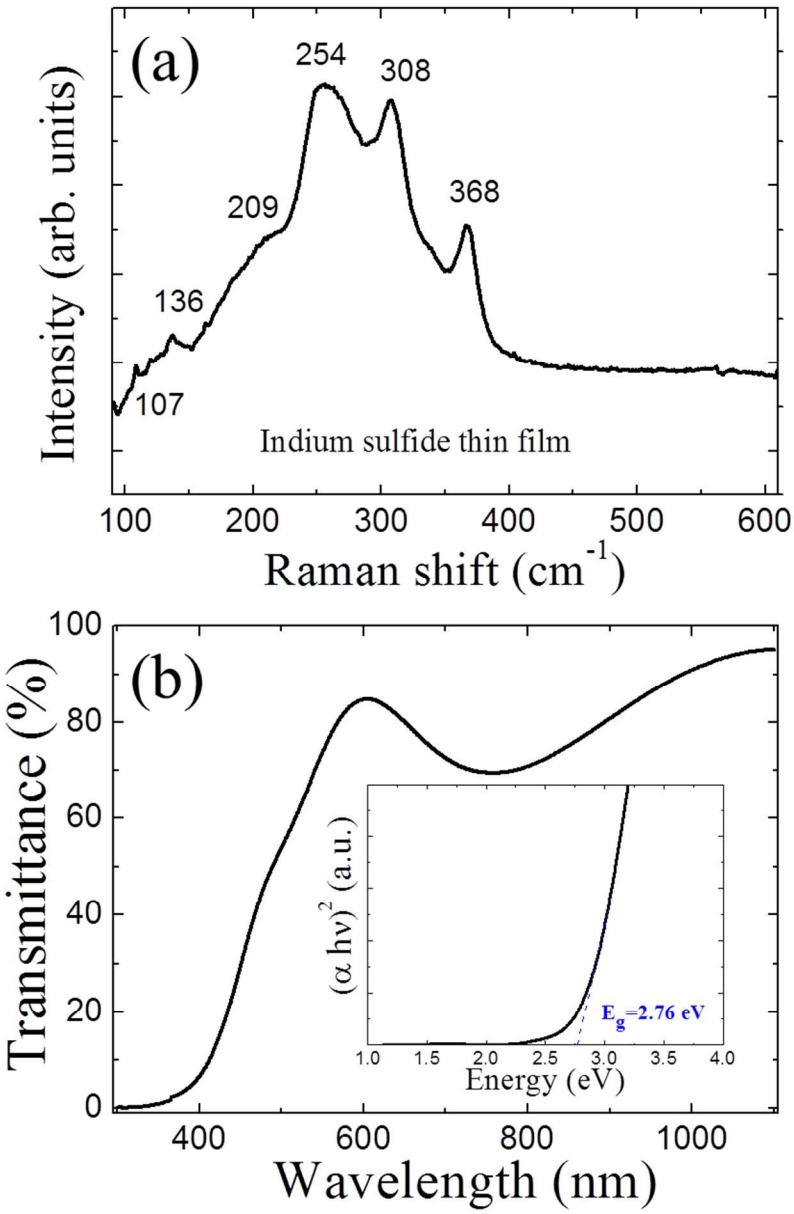

Figure S1. Raman spectrum (a) and transmittance (b) of indium sulfide (In_2S_3) buffer deposited by chemical spray pyrolysis. Inset: (b) Tauc plot for band gap estimation. These results are in good agreement to the earlier reports.[1,2]

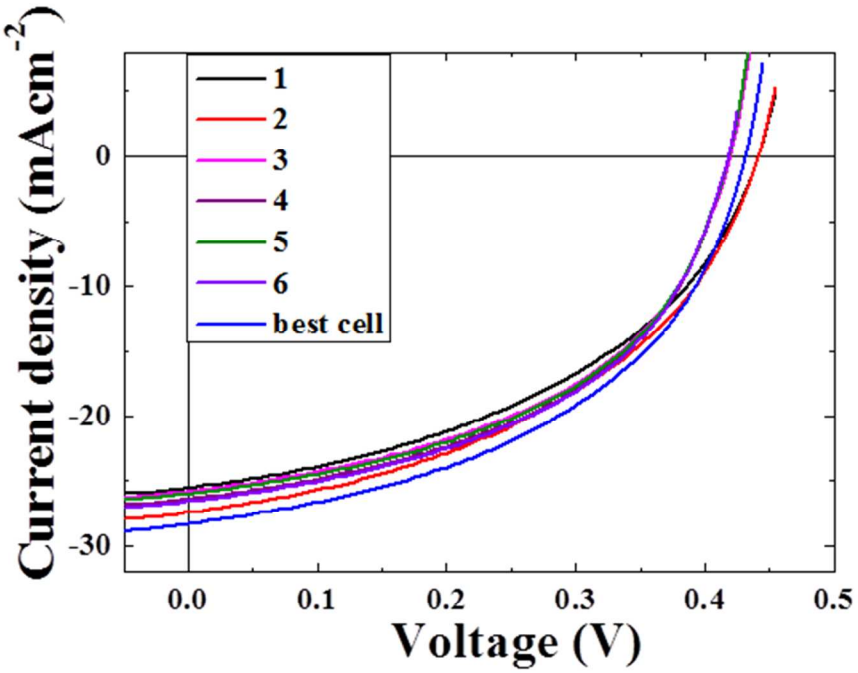

Figure S2. J-V curves of devices fabricated by same conditions as those of best solar cell device. The device parameters are corresponding cells are presented in Table S1.

Table S1. Device parameters of the corresponding cells of Figure S2.

Device parameters	1	2	3	4	5	6	Best cell	Average	Standard deviation
V_{oc} (V)	0.4411	0.4412	0.4188	0.4179	0.4176	0.4173	0.4313	0.4264	0.0112
J_{sc} (mAcm^{-2})	25.53	27.41	25.81	26.42	25.98	26.59	28.27	26.57	0.9702
FF (%)	44.34	44.81	48.46	48.85	48.86	48.73	47.07	47.30	1.968
η (%)	4.994	5.420	5.237	5.391	5.303	5.409	5.740	5.360	0.2249
R_{sh} (Ω)	640.939	641.383	736.898	747.275	778.012	762.501	632.582	705.655	64.335
R_s (Ω)	69.302	66.002	54.815	57.486	57.753	56.589	53.893	59.411	5.878

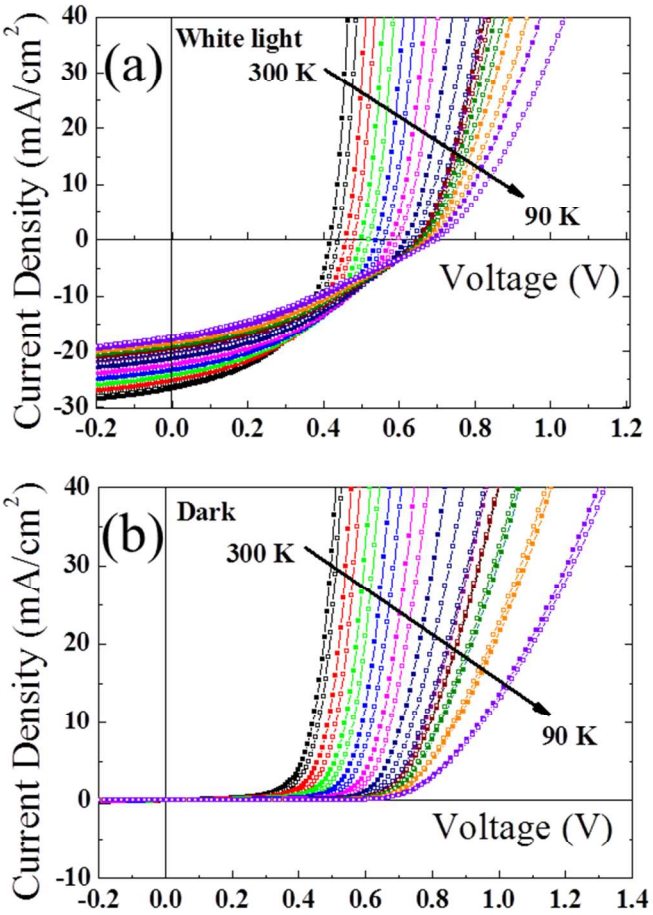

Figure S3. J-V-T characteristics of champion device under white light illumination (a) and dark condition (b) in the temperature range 300 K-90 K with $\Delta T = 10$ K as indicated by arrow points.

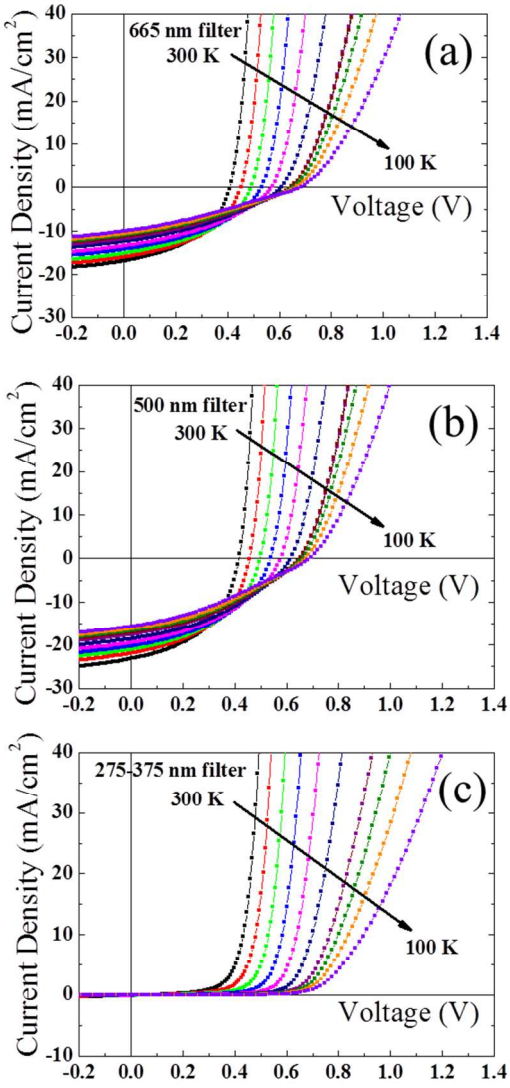

Figure S4. J-V-T characteristics under different filtered light illuminations: (a) light with wavelengths higher than 665 nm, (b) light with wavelengths higher than 500 nm, and (c) light with wavelengths in between 275-375 nm. Arrow points towards lower temperature (T= 300 K-100 K; ΔT = 20 K).

The J-V-T characteristic in the temperature range 300-100 K under filtered light illumination have been studied to get information about blue photon doping or red-kink

effect which usually occurs as consequence of interface conduction band offset. In 665 nm filter case (Fig. S3a), no carriers are generated in the In_2S_3 buffer layer (E_g = 2.76 eV, Figure S1) whereas 500 nm filter (Fig. S3b) cuts off around band gap of the buffer layer, therefore the J_{sc} value is found to be much lower in case of 665 nm filter than that of 500 nm filter compared to the white light illuminated J-V-T results. The slight loss of FF is observed toward low temperatures for J-V-T under 665 nm illuminated filter which indicates weak red-kink effect whereas the filtered light illumination study of CZTSe/CdS solar cell has been reported to have strong red-kink effect.[3] The J-V-T results with 275-375 nm filter illumination (Fig. S3c) is close to dark J-V-T results which indicated no effective contribution from the illuminated light of higher energy range than band gap of buffer layer for photo current generation. In this result, weak red-kink effect is believed to be due to freeze out of shallow accepter defect at lower temperature.

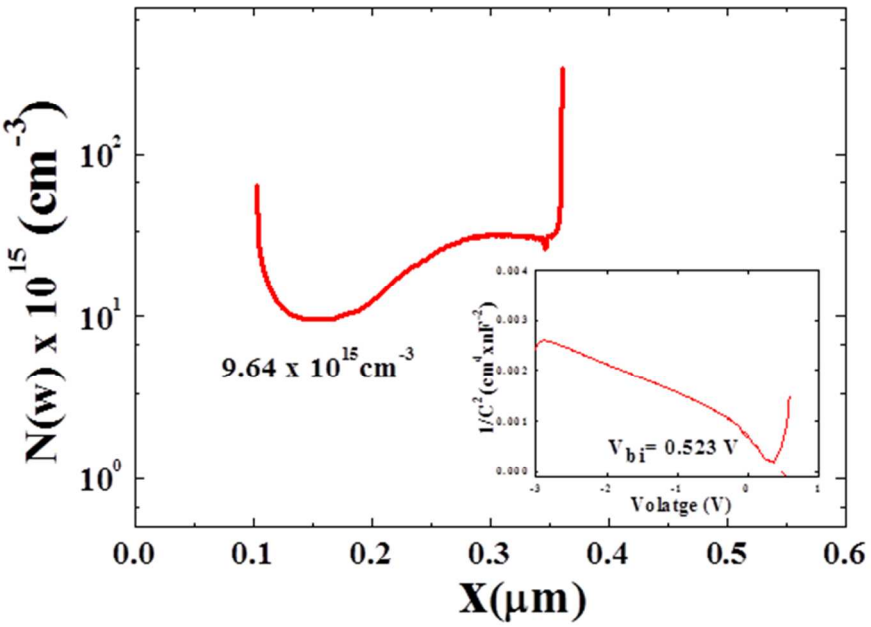

Figure S5. Charge carrier density profile determined from capacitance voltage (C-V) measurement at 90 K. Inset: Mott-Schottky plot and built-in-potential estimation.

C-V measurement was analyzed to estimate the carrier charge density and built in potential at cell junction by Mott-Schottky plot on the basis of following relation.[4,5]

$$\frac{1}{C^2} = \frac{2}{qN_a\varepsilon_o\varepsilon_s A^2}(V_{bi} - V) \qquad (1)$$

$$N_a = -\frac{2}{q\varepsilon_o\varepsilon_s A^2}\left[\frac{d}{dV}\left(\frac{1}{C^2}\right)\right]^{-1} \qquad (2)$$

where N_a is free carrier charge density, q is the fundamental charge, ε_0 is permittivity of free space, ε_s is dielectric constant, 8.6, for CZTSe[6], and A is area of the cell. Figure S5 shows the carrier density profile as function of position in absorber layer calculated using Eq. 2 which is

distributed within a certain range. The built in potential (V_{bi}) estimated by evaluating Mott-Schottky plot (Figure S5 Inset) obtained from Eq. 1 is 0.523 V.

REFERENCES

(1) Karber, E.; Otto, K.; Katerski, A.; Mere, A.; Krunks, M. Raman Spectroscopic Study of In_2S_3 Films Prepared by Spray Pyrolysis, *Mater. Sci. Semicond. Process.* **2014**, *25***,** 137–142.

(2) Otto, K.; Katerski, A.; Mere, A. Volobujeva O, Krunks M, Spray Pyrolysis Deposition of Indium Sulphide Thin Films. *Thin Solid Films* **2011**, *519*, 3055–3060.

(3) Redinger. A.; Mousel, M.; Djemour, R.; Gutay, L.; Valle, N.; Siebentritt, S. $Cu_2ZnSnSe_4$ Thin Film Solar Cells Produced via Co-evaporation and Annealing Including a $SnSe_2$ Capping Layer. *Prog. Photovoltaics: Res. Appl.* **2014**, *22*, 51–57.

(4) Abou-Ras, D.; Kirchartz, T.; Rau, U. *Advance Characterization Techniques for Thin Film Solar cell*. Wiley-VCH Verlag GmbH & Co. KGaA, Weinheim, Germany **2011**, 81-103.

(5) Heath, J. T.; Cohen, J. D.; Shafarman, W. N. Bulk and Metastable Defects in $CuIn_{1-x}Ga_xSe_2$ Thin Films Using Drive-Level Capacitance Profiling. *J. Appl. Phys.* **2004**, *95*, 100-110.

(6) Persso, C. Electronic and Optical Properties of Cu_2ZnSnS_4 and $Cu_2ZnSnSe_4$. *J. Appl. Phys.* **2010**, *107*, 0537101-0537108.